

Mitigating transmit B_1 inhomogeneity in the liver at 7T using multi-spoke parallel transmit RF pulse design

Xiaoping Wu, Sebastian Schmitter, Edward J. Auerbach, Kâmil Uğurbil, Pierre-François Van de Moortele

Center for Magnetic Resonance Research, Department of Radiology, University of Minnesota Medical School, Minneapolis, Minnesota, USA

Corresponding to: Xiaoping Wu, Ph.D. Center for Magnetic Resonance Research, University of Minnesota Medical School, 2021 6th Street S.E., Minneapolis, MN 55455, USA. Email: xiaoping.wu2010@gmail.com.

Abstract: In this work, the use of multi-spoke slice-selective parallel transmit (pTX) RF pulse was explored to address B_{1+} inhomogeneity in the largest transverse section of the liver at 7T. The impact of the number of spokes was specifically investigated, considering RF pulses consisting of 2, 3 and 4 spokes, as well as single-spoke RF pulses corresponding to static B_1 shimming. Healthy volunteers were imaged on a whole body MR scanner equipped with an eight-channel transmit system. A robust and fast transmit B_1 (B_{1+}) estimation method was employed to obtain the eight-channel B_{1+} maps within a single breath hold. Gradient echo (GRE) images of the liver were acquired using the four different RF pulses and the results were compared. The use of static B_1 shimming (i.e., 1-spoke RF pulse) resulted in partial improvement but significant signal dropouts were still observed in the target region. By comparison, the use of multi-spoke pTX RF pulse design gave rise to much improved excitation homogeneity without signal dropouts. These results demonstrate the effectiveness of multi-spoke pTX RF pulse design in B_{1+} homogenization for liver magnetic resonance imaging (MRI) at 7T. The current findings at 7T may have implications for body imaging applications in clinical settings at 3T where B_{1+} inhomogeneities are also known for degrading image quality in the torso.

Keywords: Parallel transmit (pTX); RF pulse design; transmit B_1 homogenization; ultrahigh field magnetic resonance imaging (MRI)



Submitted Jan 01, 2014. Accepted for publication Feb 26, 2014.

doi: 10.3978/j.issn.2223-4292.2014.02.06

Scan to your mobile device or view this article at: <http://www.amepc.org/qims/article/view/3431/4285>

Introduction

A straightforward principle to increase signal to noise ratio (SNR) in ^1H magnetic resonance imaging (MRI) acquisitions is to increase the main magnetic field, which determines the operating Larmor frequency. Because of this, there has been a growing interest in pursuing MRI at 7T to achieve improved spatial resolutions and/or enhanced contrast. However, technical challenges arise at such high magnetic field, including increased transmit B_1 (B_{1+}) inhomogeneity due to the shortened RF wavelength becoming similar to or smaller than the size of the imaged object, and elevated RF power deposition in tissues [i.e., specific absorption rate (SAR)] (1,2). Fast, robust and practical methods therefore must be developed to address these issues especially when considering clinical applications of body MRI at 7T (3). To date, static B_1 shimming (4), consisting of applying a

complex coefficient (denoting RF phase and magnitude modulation) specific to each individual channel of a transmit array, has successfully been used to address these problems at 7T in several targets including heart (5), prostate (6), kidneys (7) and hips (8). However, obtaining a uniform B_{1+} field at 7T using static B_1 shimming over the longest dimension of large organs such as the liver is extremely challenging (9), if not impossible. Furthermore, such B_1 shim solutions typically come at the cost of very low RF efficiency due to high levels of destructive interferences (10), yielding SAR values beyond acceptable limits.

On the other hand, parallel transmit (pTX) (11-15) combined with multi-spoke (16,17) or k_1 -point (18) RF pulses allows for larger degrees of freedom to address B_{1+} inhomogeneity and holds great potentials to create a homogeneous excitation even over a large target. Whereas

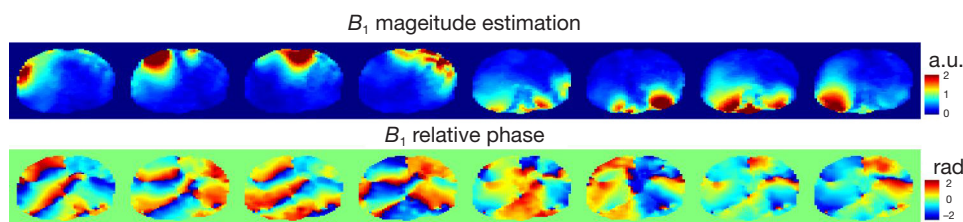


Figure 1 Transmit B_1 magnitude estimation (top row, arbitrary units) and relative phases (bottom row) in the human body for the 8-channel RF array.

some studies have shown that liver imaging at 7T could be improved either by using a single static B_1 shimming solution (19) or by collecting two interleaved datasets each obtained with a distinct static B_1 shimming solution (20), our interest was to further improve excitation homogeneity, within a single image acquisition, through the largest axial section of the liver at 7T. To this end, we employed multi-spoke pTX RF pulse design previously demonstrated capable of providing satisfactory B_1+ homogenization for slice-selective RF excitation in brain imaging at 7T (21) and above (22), as well as we investigated the impact of the number of spokes on RF excitation performance by comparing liver images obtained using different pulses. A robust multi-channel B_1+ mapping technique (23) suitable to satisfy speed and robustness requirements for clinical applications was utilized, enabling B_1+ mapping of eight transmit channels to be accomplished within a single breath hold. Some initial results of this study have been partially reported in the format of a conference abstract (24); in the current paper we present a more complete and detailed report of this work together with more advanced results.

Materials and methods

All experiments were performed on a 7T, 90-cm-bore MR scanner (Magnex, Oxford, UK) equipped with whole-body gradient coils with a maximum gradient strength of 40 mT/m and a maximum slew rate of 170 T/m/s. The scanner was driven by a Siemens prototype pTX system (Siemens, Erlangen, Germany) with eight independent RF transmit channels, each powered by a 1 kW RF amplifier (CPC, Hauppauge, NY, USA). An eight-channel stripline body array (25) was used for both RF transmission and reception, which consisted of two (anterior and posterior) plates each with four coil elements.

In addition to the standard MR console RF power monitoring system measuring the forward and reflected

power for each of the eight transmit channels, a similar RF power monitoring system was developed in-house. The eight RF power amplifiers were equipped with a directional coupler providing an attenuated version of the output waveform, of which the power envelope was continuously sampled by a calibrated ADC board. The system was maintaining a 10-sec and 6-min moving average and would immediately disable all RF amplifiers and terminate the MR pulse sequence if the mean power exceeded a predefined wattage threshold. Thresholds were conservatively determined against the worst-case scenario, assuming all RF coil electric fields to add constructively in the sample.

All computations, including RF pulse design and Bloch simulations, were conducted in Matlab (MathWorks, Natick, MA, USA). Healthy volunteers who signed an IRB-approved consent were recruited for this study. Representative results are shown here.

Transmit B_1 , receive B_1 and ΔB_0 field mapping

In vivo complex B_1+ maps (Figure 1) for the eight transmit channels were obtained using an ultra-fast multi-channel B_1+ estimation technique (23) based on a calibration scan acquired during a single breath hold. With this method, the B_1+ estimation for individual transmit channels was derived based on a series of gradient echo (GRE) images, acquired in the small flip angle regime by transmitting excitation RF power through one channel at a time. The GRE images were obtained with TR/TE = 20/3.7 ms, slice thickness = 5 mm, field of view = 45×45 cm² and matrix size = 128×64. The total acquisition time was 14 seconds. Figure 1 shows the resulting B_1+ estimation for the eight-channel body array utilized in this study. Receive B_1 maps of all channels were also estimated using the same series of GRE images.

In addition, susceptibility induced ΔB_0 maps were derived from GRE images acquired at two TE's (TE1/TE2 = 5/6 ms) and were incorporated into RF pulse design to minimize

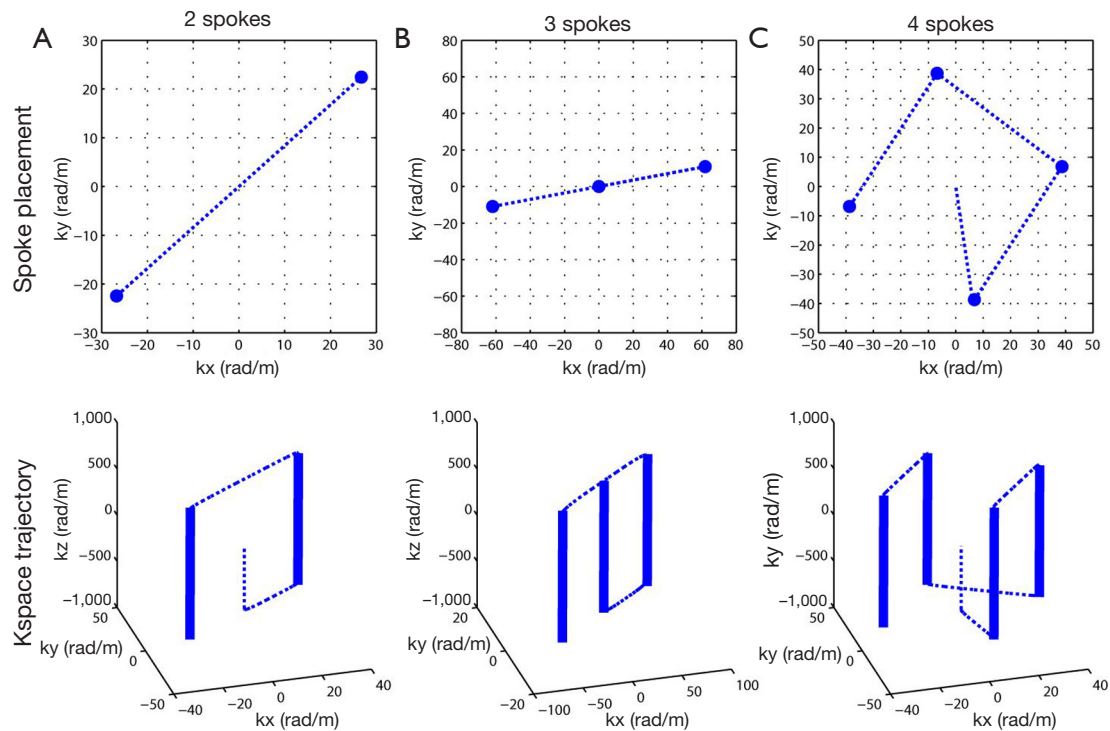


Figure 2 Example k -space trajectory designs for 2 (A), 3 (B) and 4 (C) spokes for one human subject. The spokes were constrained to be symmetrically placed around the origin in the k_x - k_y plane. In addition, the placement was optimized over a grid defined by different rotation angles ranging from 0 to 170 degrees in steps of 10 degrees and by different separation distances ($\Delta k = 1/\text{FOV}$) with FOV ranging from 8 to 18 cm in steps of 2 cm.

off-resonance effects (13-15). Both ΔB_0 and B_{1+} maps were down-sampled for the subsequent RF pulse design.

RF pulse design

Slice-selective multi-spoke pTX RF pulses were designed with 3D spoke trajectories aiming at creating a uniform excitation within a region of interest (ROI) manually drawn so as to include the liver tissues in an axial view positioned at the largest transverse section of the organ. All RF pulses were designed with a 128×64 in-plane matrix size. For improved excitation performance, the magnitude and phase modulations of the RF sub-pulse for each individual spoke and each individual RF channel were calculated based on the magnitude least squares optimization (26) with total RF power regularization and with the subject-specific spoke placement optimized in a way similar to that in Reference (21). Figure 2 displays the resulting k -space trajectories with 2, 3 and 4 spokes optimized for one subject. RF sub-pulses were Gaussian shaped with a time-bandwidth-product of 2 and were 0.5 ms in length.

Trapezoidal slice-selective gradients were designed for a slice thickness of 5 mm with the maximum gradient strength being 22 mT/m and the maximum slew rate 140 mT/m/s. For comparison, static B_1 shimming pulses were also calculated by positioning a single spoke at the k -space origin. The total pulse durations including gradient ramps andrewinder were 1.84, 2.98, 4.12 and 5.26 ms for static B_1 shim (i.e., single spoke), 2-, 3- and 4-spoke pulses, respectively.

Parallel transmit experiment and simulation

Images of the liver obtained with different RF pulses were compared. Images were first acquired using a modified 3D GRE pulse sequence where the traditional excitation module was replaced by the 3D spoke RF excitation. The relevant imaging parameters were as follows: $\text{FOV} = 450 \times 366 \times 32 \text{ mm}^3$, matrix size $= 256 \times 208 \times 32$, $\text{TR/TE} = 11/1.66 \text{ ms}$, GRAPPA $= 2$ and partial Fourier $= 6/8$. The acquisition time was 23 seconds. In order to retain signal variations mainly due to B_{1+} , those images were further divided by the root of sum of squares of

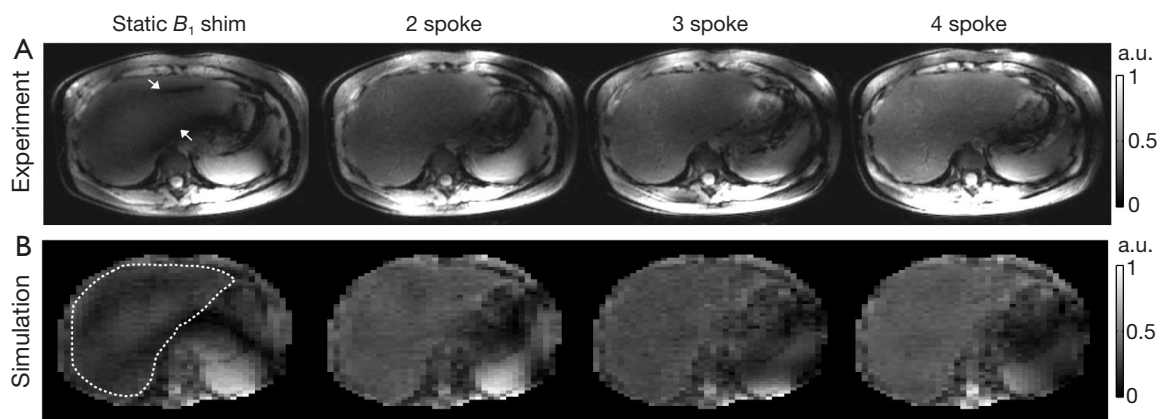


Figure 3 Comparison of static B_1 shimming and multi-spoke pTX pulse design when used to mitigate B_1+ inhomogeneity in liver MRI at 7T. (A) central axial views (1 mm thick) of 3D GRE datasets acquired in one subject using four RF pulse designs. Note that two dark stripes (as indicated by white arrows) observed with the static B_1 shimming solution were effectively removed by using multi-spoke pTX RF pulses; (B) corresponding Bloch simulations of the transverse magnetization using the same pulses as in (A). The white dotted loop in the leftmost image indicates the ROI covering the liver area for which B_1+ homogenization was intended. Note the good agreement between experiments and simulations in terms of excitation pattern characteristics.

the eight estimated receive B_1 (i.e., B_{1-}) maps from the raw images.

Another 2D GRE image was also obtained using a 3-spoke pulse with high in-plane resolutions. In this case, the image was acquired with $\text{FOV} = 380 \times 285 \text{ mm}^2$, in-plane resolution $= 0.8 \times 0.8 \text{ mm}^2$, $\text{TR/TE} = 14/1.66 \text{ ms}$, averages $= 10$, GRAPPA $= 2$ and partial Fourier $= 6/8$. The acquisition time was 21 seconds. All 2D and 3D acquisitions were completed during a single breath hold.

In order to verify the fidelity of RF excitation profiles, Bloch simulations of the transverse magnetization distributions were conducted using the designed RF pulses along with the measured B_1+ and ΔB_0 maps. The transverse magnetization was defined on a 128×64 grid covering a $45 \times 45 \text{ cm}^2$ region to match closely the experimental settings. In all simulations, the magnetization at equilibrium was assumed to be uniform over space, and no relaxation or diffusion effects were considered.

Results

As seen in *Figure 3A* showing liver images obtained in one subject, pTX with multi-spoke pulse design significantly improved flip angle homogeneity through the liver as compared to static B_1 shimming (i.e., 1-spoke pulse design); the two evident dark bands of signal dropouts present in the image obtained using static B_1 shimming were effectively removed by applying multi-spoke pTX pulses. In addition,

excitation profile predictions based on Bloch simulations (*Figure 3B*) using the same RF pulses consistently provided fairly consistent results when compared with experimental results as shown in *Figure 3A*; note however that in *Figure 3A* the experimental images were still modulated by the receive sensitivity profile of the coils. When these results were further corrected for the receive sensitivity profile of the coil array, which typically consists of a pattern (easily recognized in *Figure 3A*) that includes a brighter signal in the periphery than in the center of the torso, experimental findings (*Figure 4*) and Bloch equation based simulations (*Figure 3B*) were even more consistent with each other.

The expected Gaussian shape of the slice excitation profile was verified with the modified 3D GRE sequence, as can be seen in *Figure 5A* showing the slice profile obtained in another subject with a 3-spoke pTX RF pulse, derived either from experimental measurement or from Bloch simulations, with a high level of consistency between the two plots. Note that these plots correspond to a projection of the liver 3D image along the slice selection axis (i.e., the Z-axis).

In order to achieve higher in-plane spatial resolution ($0.8 \times 0.8 \text{ mm}^2$) while keeping total acquisition time within a single breath hold, single-slice 2D GRE images were also acquired in the same subject while using the 3-spoke excitation RF pulse. The corresponding result, shown in *Figure 5B*, demonstrates satisfactory excitation through the ROI over the transverse section of the liver, even though,

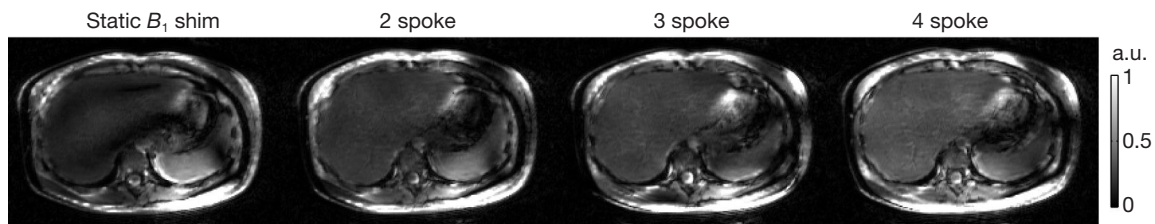


Figure 4 Experimental results: excitation profiles corresponding to the four RF pulse designs as illustrated in *Figure 3A*. These images were obtained by dividing out the root of sum of squares of the eight receive B1 profiles from the images shown in *Figure 3A*. Note the increased uniformity of signal intensity in the liver over the area corresponding to the ROI shown in *Figure 3B*.

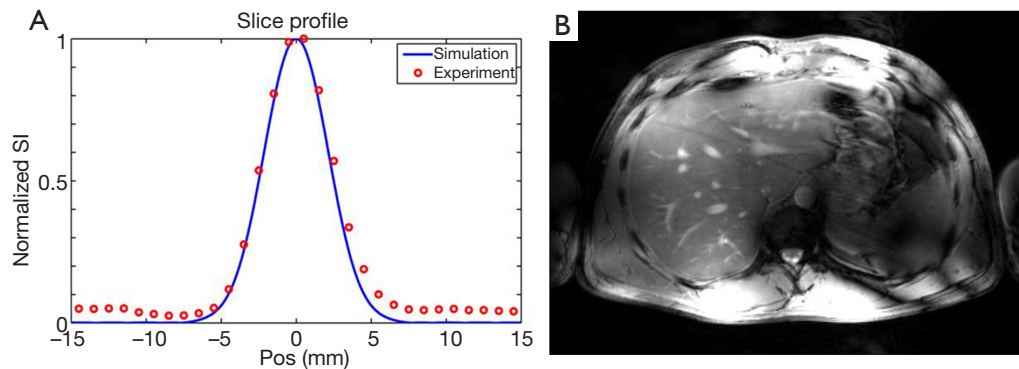


Figure 5 Slice selectivity verification and high resolution imaging using multi-spoke pTX RF pulses. (A) experimental (circles) and simulated (curve) slice profiles of a 3-spoke RF pulse designed for another subject. The experimental slice profile corresponds to the projection of a 3D GRE dataset on the slice selective axis (i.e., Z-axis). The numerical prediction was based on 1D Bloch simulations. Note the high consistency between prediction and experiment, especially within the excited slice; (B) higher spatial resolution obtained in a 2D GRE image using the same 3-spoke pulse. Relevant imaging parameters were FOV = 38×28.5 cm², resolution = 0.8 mm isotropic, TR/TE = 14/1.66 ms, averages = 10, GRAPPA = 2 and partial Fourier = 6/8. Total acquisition time was 21 s. Note the higher conspicuity of liver vasculature.

as expected, image magnitude homogeneity was altered to a certain degree by the receive sensitivity profile (similar to that in *Figure 3A*, third column), while providing higher conspicuity of anatomical and vascular structures.

Discussion

In this study we have demonstrated that slice selective multi-spoke pTX RF pulses designed with 3D spoke trajectories can be used to substantially improve excitation homogeneity over an entire transverse plane of the liver, when compared with static B_1 shimming (i.e., 1-spoke) results, and therefore hold great potentials for future clinical applications. Our study also indicates that the ultra-fast B_1+ estimation method based on small flip angle GRE images presents several advantages that are especially significant when used to obtain B_1+ maps for multiple channels in

the torso at 7T. These advantages include robustness against susceptibility induced B_0 variations (standard GRE sequence) and against physiological motion (B_1+ maps for eight channels obtained in a single breath hold acquisition), minimum RF power requirement and minimum SAR levels (small flip angles). Even though the B_1+ maps estimated with this method alone are partially biased by the square root of proton density profile, they do provide satisfactory results for designing multi-spoke pTX RF pulses (as long as ΔB_0 maps are concomitantly acquired). A scaling factor required to convert estimated maps into absolute B_1+ values could be obtained with an additional calibration scan if needed (23).

It is interesting to observe that, although excitation homogeneity keeps improving as the number of spokes increases, most of the improvement can already be achieved with 2-spoke pTX RF pulse design with only a smaller benefit added when using 3- or 4-spoke pulses. Similar observations

were also obtained in a recently published work investigating the use of slice-selective multi-spoke pTX pulses in cardiac imaging at 7T (27). The optimal number of spokes however will need to be revisited when utilizing a different number of RF coil elements as well as when considering a 3D ROI rather than a 2D slice selective target.

Although it is well known that at 7T large B_1+ variations are a serious challenge for torso imaging, similar problems actually also occur, at a smaller scale, at 3T. Considering the growing interest among the main clinical MR scanner vendors in building multi-channel transmit systems for clinical 3T scanners, we anticipate that our current findings may also result in significant applications for clinical settings at 3T.

In summary, we have demonstrated the utility of multi-spoke slice selective pTX RF pulse design in producing a more homogeneous RF excitation in the liver at 7T, allowing for imaging the largest transverse section of the liver without significant signal dropouts despite of the presence of severe transmit B_1 inhomogeneity.

Acknowledgements

The authors would like to thank Dr. Carl Snyder for building the body array, and Drs. Greg Metzger and Lance DelaBarre for assistance with the experimental setup. This work was supported by the KECK Foundation and NIH grants including EB006835, PAR-02-010, EB007327, P41 RR008079, P30 NS057091 and S10 RR026783.

Disclosure: The authors declare no conflict of interest.

References

- Collins CM, Yang QX, Wang JH, et al. Different excitation and reception distributions with a single-loop transmit-receive surface coil near a head-sized spherical phantom at 300 MHz. *Magn Reson Med* 2002;47:1026-8.
- Vaughan JT, Garwood M, Collins CM, et al. 7T vs. 4T: RF power, homogeneity, and signal-to-noise comparison in head images. *Magn Reson Med* 2001;46:24-30.
- Vaughan JT, Snyder CJ, DelaBarre LJ, et al. Whole-body imaging at 7T: preliminary results. *Magn Reson Med* 2009;61:244-8.
- Mao W, Smith MB, Collins CM. Exploring the limits of RF shimming for high-field MRI of the human head. *Magn Reson Med* 2006;56:918-22.
- Snyder CJ, DelaBarre L, Metzger GJ, et al. Initial results of cardiac imaging at 7 Tesla. *Magn Reson Med* 2009;61:517-24.
- Metzger GJ, Snyder C, Akgun C, et al. Local B_1+ shimming for prostate imaging with transceiver arrays at 7T based on subject-dependent transmit phase measurements. *Magn Reson Med* 2008;59:396-409.
- Metzger GJ, Auerbach EJ, Akgun C, et al. Dynamically applied B_1+ shimming solutions for non-contrast enhanced renal angiography at 7.0 Tesla. *Magn Reson Med* 2013;69:114-26.
- Ellermann J, Goerke U, Morgan P, et al. Simultaneous bilateral hip joint imaging at 7 Tesla using fast transmit $B(1)$ shimming methods and multichannel transmission - a feasibility study. *NMR Biomed* 2012;25:1202-8.
- Snyder AL, Snyder CJ, DelaBarre L, et al. Preliminary experience with liver MRI and 1H MRS at 7 Tesla. *Proc Intl Soc Mag Reson Med* 2007;15:729.
- Van de Moortele PF, Akgun C, Adriany G, et al. $B(1)$ destructive interferences and spatial phase patterns at 7 T with a head transceiver array coil. *Magn Reson Med* 2005;54:1503-18.
- Katscher U, Börnert P, Leussler C, et al. Transmit SENSE. *Magn Reson Med* 2003;49:144-50.
- Zhu Y. Parallel excitation with an array of transmit coils. *Magn Reson Med* 2004;51:775-84.
- Ullmann P, Junge S, Wick M, et al. Experimental analysis of parallel excitation using dedicated coil setups and simultaneous RF transmission on multiple channels. *Magn Reson Med* 2005;54:994-1001.
- Grissom W, Yip CY, Zhang Z, et al. Spatial domain method for the design of RF pulses in multicoil parallel excitation. *Magn Reson Med* 2006;56:620-9.
- Setsoompop K, Wald LL, Alagappan V, et al. Parallel RF transmission with eight channels at 3 Tesla. *Magn Reson Med* 2006;56:1163-71.
- Saekho S, Yip CY, Noll DC, et al. Fast-kz three-dimensional tailored radiofrequency pulse for reduced B_1 inhomogeneity. *Magn Reson Med* 2006;55:719-24.
- Zhang Z, Yip CY, Grissom W, et al. Reduction of transmitter B_1 inhomogeneity with transmit SENSE slice-select pulses. *Magn Reson Med* 2007;57:842-7.
- Cloos MA, Boulant N, Luong M, et al. kT -points: short three-dimensional tailored RF pulses for flip-angle homogenization over an extended volume. *Magn Reson Med* 2012;67:72-80.
- Umutlu L, Bitz AK, Maderwald S, et al. Contrast-enhanced ultra-high-field liver MRI: a feasibility trial. *Eur J Radiol* 2013;82:760-7.
- Orzada S, Maderwald S, Poser BA, et al. RF excitation using time interleaved acquisition of modes (TIAMO) to

- address B1 inhomogeneity in high-field MRI. *Magn Reson Med* 2010;64:327-33.
21. Setsompop K, Alagappan V, Gagoski B, et al. Slice-selective RF pulses for in vivo B1+ inhomogeneity mitigation at 7 tesla using parallel RF excitation with a 16-element coil. *Magn Reson Med* 2008;60:1422-32.
 22. Wu X, Adriany G, Ugurbil K, et al. Correcting for strong eddy current induced B0 modulation enables two-spoke RF pulse design with parallel transmission: demonstration at 9.4T in the human brain. *PLoS One* 2013;8:e78078.
 23. Van de Moortele PF, Ugurbil K. Very fast multi channel B1 calibration at high field in the small flip angle regime. *Proc Intl Soc Mag Reson Med* 2009;17:367.
 24. Wu X, Schmitter S, Auerbach EJ, et al. Parallel transmission in liver MRI at 7T: initial results. *Proc Intl Soc Mag Reson Med* 2011;19:2940.
 25. Snyder CJ, DelaBarre L, van De Moortele PF, et al. Stripline/TEM transceiver array for 7T body imaging. *Proc Intl Soc Mag Reson Med* 2007;15:164.
 26. Setsompop K, Wald LL, Alagappan V, et al. Magnitude least squares optimization for parallel radio frequency excitation design demonstrated at 7 Tesla with eight channels. *Magn Reson Med* 2008;59:908-15.
 27. Schmitter S, DelaBarre L, Wu X, et al. Cardiac imaging at 7 Tesla: Single- and two-spoke radiofrequency pulse design with 16-channel parallel excitation. *Magn Reson Med* 2013;70:1210-9.

Cite this article as: Wu X, Schmitter S, Auerbach EJ, Ugurbil K, Van de Moortele PF. Mitigating transmit B_1 inhomogeneity in the liver at 7T using multi-spoke parallel transmit RF pulse design. *Quant Imaging Med Surg* 2014;4(1):4-10. doi: 10.3978/j.issn.2223-4292.2014.02.06